
# NAVAL POSTGRADUATE SCHOOL

**MONTEREY, CALIFORNIA**

# THESIS

**FLOW STUDY OF A NOVEL IONIZER CONFIGURATION WITH TESTING APPARATUS**

by

John David Armstrong

March 2008

Thesis Advisor: Oscar Biblarz
Co-Advisor: Jose Sinibaldi

**Approved for public release; distribution is unlimited**

THIS PAGE INTENTIONALLY LEFT BLANK

| REPORT DOCUMENTATION PAGE | | | Form Approved OMB No. 0704-0188 |
|---|---|---|---|
| Public reporting burden for this collection of information is estimated to average 1 hour per response, including the time for reviewing instruction, searching existing data sources, gathering and maintaining the data needed, and completing and reviewing the collection of information. Send comments regarding this burden estimate or any other aspect of this collection of information, including suggestions for reducing this burden, to Washington headquarters Services, Directorate for Information Operations and Reports, 1215 Jefferson Davis Highway, Suite 1204, Arlington, VA 22202-4302, and to the Office of Management and Budget, Paperwork Reduction Project (0704-0188) Washington DC 20503. | | | |
| **1. AGENCY USE ONLY** ***(Leave blank)*** | **2. REPORT DATE** March 2008 | **3. REPORT TYPE AND DATES COVERED** Master's Thesis | |
| **4. TITLE AND SUBTITLE** Flow Study of a Novel Ionizer Configuration with Testing Apparatus | | **5. FUNDING NUMBERS** | |
| **6. AUTHOR(S)** | | | |
| **7. PERFORMING ORGANIZATION NAME(S) AND ADDRESS(ES)** Naval Postgraduate School Monterey, CA 93943-5000 | | **8. PERFORMING ORGANIZATION REPORT NUMBER** | |
| **9. SPONSORING /MONITORING AGENCY NAME(S) AND ADDRESS(ES)** N/A | | **10. SPONSORING/MONITORING AGENCY REPORT NUMBER** N/A | |
| **11. SUPPLEMENTARY NOTES** The views expressed in this thesis are those of the author and do not reflect the official policy or position of the Department of Defense or the U.S. Government. | | | |
| **12a. DISTRIBUTION / AVAILABILITY STATEMENT** Approved for public release; distribution is unlimited | | **12b. DISTRIBUTION CODE** | |


**13. ABSTRACT** (maximum 200 words)

Micro-satellites require a propulsion system that minimizes mass and size while maximizing performance. Ion propulsion engines may be the most scalable pending reductions in ionizer size. This work explores a new ionization chamber concept.

This thesis reports on the ionization of Argon, an alternative propellant to Xenon, which has been achieved at relatively low voltages with locally designed and manufactured Micro-Structured Electrode (MSE) Arrays. Testing was done with the gas flowing through the array holes, simulating the actual space environment as in an operating ion thruster. With argon flowing, breakdown has been achieved at voltages between 230 and 350 volts depending on chamber pressure, and array insulation thickness and hole size. The breakdown voltage in argon gas was higher (between 15 and 100 volts) with the flow than that without for the same wafer, and always higher for the smaller (0.127 mm vs. 0.381 mm) insulation thickness tested. No breakdown was observed when the cathode was located upstream.


| **14. SUBJECT TERMS** Space Propulsion, Ion Thruster, Ionizer Chamber | | | **15. NUMBER OF PAGES** 83 |
|---|---|---|---|
| | | | **16. PRICE CODE** |
| **17. SECURITY CLASSIFICATION OF REPORT** Unclassified | **18. SECURITY CLASSIFICATION OF THIS PAGE** Unclassified | **19. SECURITY CLASSIFICATION OF ABSTRACT** Unclassified | **20. LIMITATION OF ABSTRACT** UU |

NSN 7540-01-280-5500 Standard Form 298 (Rev. 2-89)
Prescribed by ANSI Std. 239-18

THIS PAGE INTENTIONALLY LEFT BLANK

**Approved for public release; distribution is unlimited**

# FLOW STUDY OF A NOVEL IONIZER CONFIGURATION WITH TESTING APPARATUS

John D. Armstrong
Lieutenant, United States Navy
B.S., United States Naval Academy, 2000

Submitted in partial fulfillment of the
requirements for the degree of

**MASTER OF SCIENCE IN ASTRONAUTICAL ENGINEERING**

from the

**NAVAL POSTGRADUATE SCHOOL**
**March 2008**

Author: John D. Armstrong

Approved by: Oscar Biblarz
Thesis Advisor

Jose O. Sinibaldi
Co-Advisor

Anthony J. Healy
Chairman, Department of Mechanical and Astronautical Engineering

THIS PAGE INTENTIONALLY LEFT BLANK

# ABSTRACT

Micro-satellites require a propulsion system that minimizes mass and size while maximizing performance. Ion propulsion engines may be the most scalable pending reductions in ionizer size. This work explores a new ionization chamber concept.

This thesis reports on the ionization of Argon, an alternative propellant to Xenon, which has been achieved at relatively low voltages with locally designed and manufactured Micro-Structured Electrode (MSE) Arrays. Testing was done with the gas flowing through the array holes, simulating the actual space environment as in an operating ion thruster. With argon flowing, breakdown has been achieved at voltages between 230 and 350 volts depending on chamber pressure, and array insulation thickness and hole size. The breakdown voltage in argon gas was higher (between 15 and 100 volts) with the flow than that without for the same wafer, and always higher for the smaller (0.127 mm vs. 0.381 mm) insulation thickness tested. No breakdown was observed when the cathode was located upstream.

THIS PAGE INTENTIONALLY LEFT BLANK

# TABLE OF CONTENTS

# LIST OF FIGURES

THIS PAGE INTENTIONALLY LEFT BLANK

# LIST OF TABLES

THIS PAGE INTENTIONALLY LEFT BLANK

# ACKNOWLEDGMENTS

I would like to take the opportunity to thank the following individuals and groups:

God the creator and foundation of all things, without whom the world and science would cease to be; Messieurs Don Snyder, Samuel Barone, and George Jaksha of the Physics Department for their invaluable technical assistance with the vacuum chamber, computer data gathering and mounting/flow assembly; Professors Oscar Biblarz and Jose Sinibaldi for their knowledge and guidance; Frank Perry Jr. and Jason Cooper for their advice and guidance prior to their graduation: The SSAG for providing research funds to upgrade the testing system, and my wife Coreyanne and children Patience, Gabriel, and Liesl who have been supremely supportive of my task here and in my service in the Military in general.

Without the support of these this would not have been possible.

THIS PAGE INTENTIONALLY LEFT BLANK

# I. INTRODUCTION

## A. ION ENGINE HISTORY

Ion engines theory was developed by German scientists during the 1930s. Due to Germany's interest in weaponry vice space rockets these theories remained untested. German scientists that were brought to the United States were able to further work the ion propulsion theories. The advancement in the theories created interest from the Army Ballistic Missile Agency which initiated a contract with industry to study ion propulsion in 1958. This study resulted in 0.1 pound-thrust ion engine developed by Hughes Research Laboratory. Further study was not continued due to the Apollo program, not until the 1990's was continued study and testing of ion engines done [1,2].

The NASA solar Electric Power Technology Applications Readiness project reinvigorated the study of ion propulsion. One project began using xenon propellant within an ion engine, and in 1996 a test engine using Xenon was built and run for over 8000 hours, making ion thrusters reasonable alternatives to conventional chemical propulsion for space-craft thrusters. Deep Space 1 validated the results of this in space where a xenon fueled ion engine was powered for over 678 days and accelerated the space craft over 4.3 km/sec (9600 miles/hour) all using less than 74 kg (163 pounds) of xenon fuel [1].

## B. ION ENGINE OPERATION

Ion thrusters utilize a collimated beam on ions to create thrust. These ions are created from inert gases that are the propellant. The majority of thrusters use xenon gas. The propellant in injected into an ionization chamber where it undergoes ionization and is accelerated through another chamber and then out the thruster where it is combined with electrons to neutralize the ions as they exhaust. This design allows for maximum ionization of the gas and therefore maximizes the thrust from the fuel see Figure 1[3].

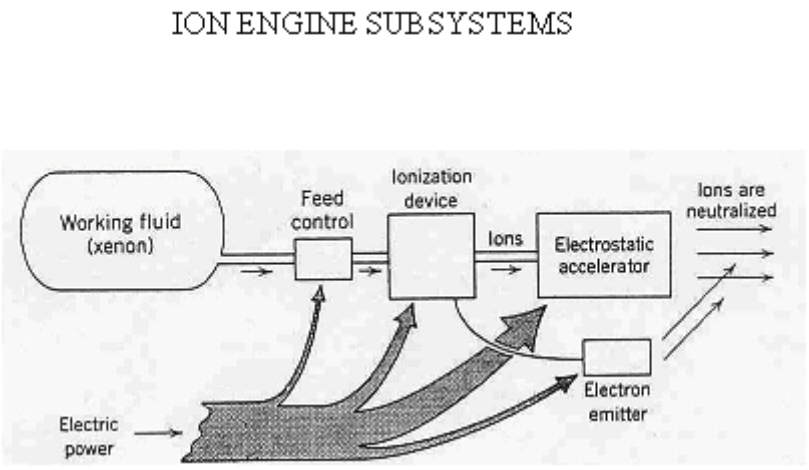


Figure 1. Ion Engine Subsystems (From 3.)

The ion thruster emits electrons at the discharge cathode, located in the center of the engine's ionizer. The electrons are attracted to the chamber walls, which are charged to a positive voltage by the thruster's power supply.

These electrons are forced to gyrate in the ionization chamber by the use of high-strength magnets. These electrons ionize the propellant throughout this process. The length of time the electrons spend in the chamber is directly proportional to the amount of propellant; residence time, increases the ionization efficiency.

At the downstream end of the ionizer are electrodes which create the electric field required to accelerate the ions, called ion optics, grids, or mask. Each electrode contains thousands of parallel coaxial apertures. The sets of apertures act as a lens to electrically focus the ions through the mask.

A two-electrode system is most commonly used in ion thrusters, where the upstream electrode is charged highly positive and the downstream electrode highly negative. Since the ions are generated in a region of high positive potential and the accelerator grid is a negative potential the ions are attracted to the accelerator grid and then are focused out the mask creating thousands of ion jets at the discharge. This stream of charged particles is called the ion beam. The thrust produced is due to the momentum gained by the ions accelerated through the accelerator grid. The exhaust velocity of the ions in the beam is proportional to the voltage applied to the optics, the charge and the molecular mass of the ions.

The ion thruster generates a very large amount of positive ions and if nothing was done to neutralize these, the thruster and spacecraft would develop a large negative charge, therefore an equal number of electrons are discharged into the exhaust beam to neutralize the ions.

This is done using a second hollow cathode called the neutralizer; the whole operation is depicted in Figure 2.

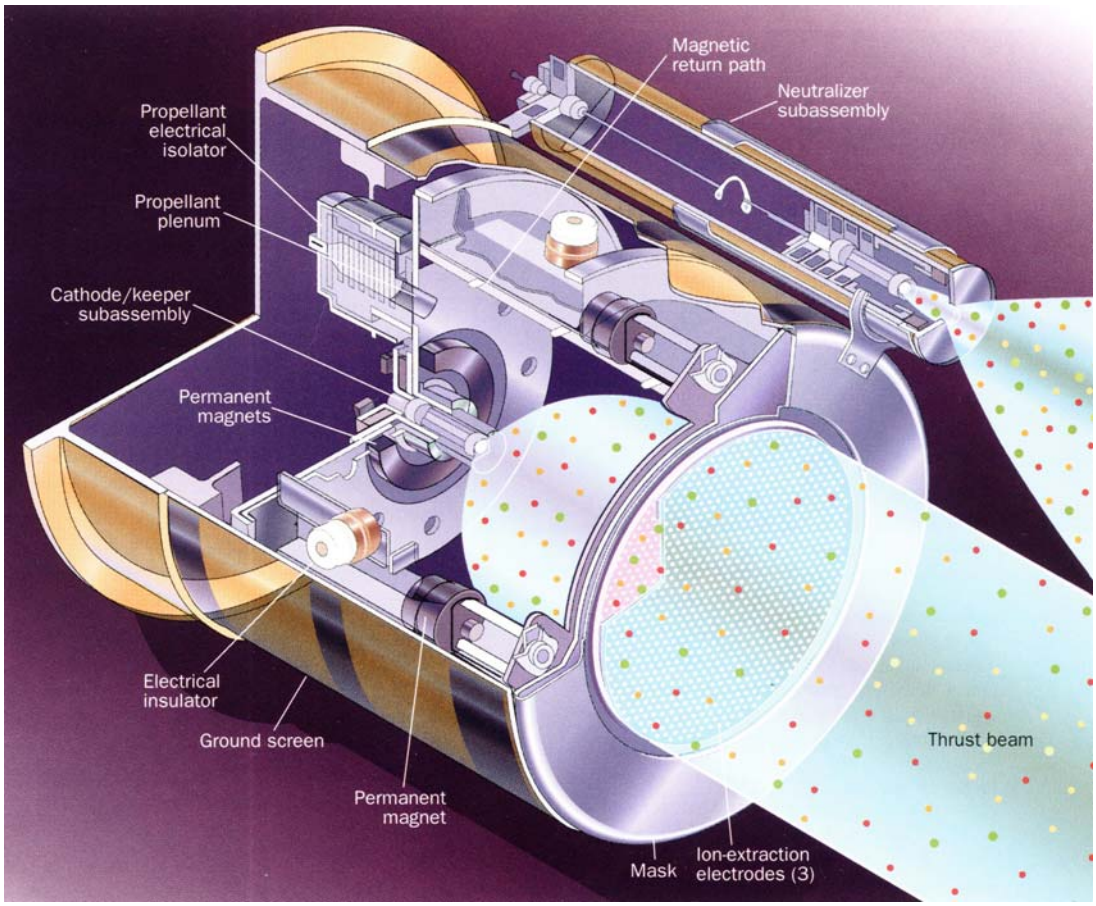


Figure 2. Ion Thruster Operation (From 4.)

An ion propulsion system requires a power source, power processing unit, propellant management system, control computer, beside the ion thruster. Any source of power may be used for the power system, but nuclear or solar are the primary options. The power processing unit converts the electrical power from the power source into the correct voltages and currents for the components in the thruster. The propellant management system regulates the flow of

propellant gas from the tank to the thruster. The control computer monitors performance and controls it accordingly. The ion thruster operates as previously discussed to generate thrust for the engine [2].

Ion thrusters are capable of propelling a spacecraft up to 90,000 meters per second with a much smaller fraction of propellant than conventional chemical thrusters. This large delta v capability with lower propellant mass is achieved with low thrust but very high specific impulse ($I_{SP}$) [1].

Modern ion thrusters deliver fractions of a Newton of thrust typically between 100mN to 500mN. To achieve a desired velocity change using such low thrust the engine must be operated for a long period of time. Because the ion thruster uses inert gas for its propellant it is inherently less risky due to the elimination of explosive risk that is associated with chemical propulsion. Xenon is usually used, but Argon and Krypton may be viable alternatives [3].

## C. APPROACH

Ion propulsion is one of several methods used for orbital maintenance and interplanetary applications. The Hall thruster's has achieved much acclaim in these areas of propulsion and caused ion propulsion technology to take a lesser role in research and development, due to the Hall thrusters adaptability to differing applications, however, ion propulsion technologies should not be ignored. Currently xenon has been used as the fuel for most ion engines due to high molecular mass and therefore greater momentum and thrust, but this is an expensive gas.

Using more common inert gases such as argon could reduce the cost of the ion engine and make it a more attractive alternative [5].

Additionally, current ionizer designs in ion engines may have reached their miniaturization limit. In order for these engines to be a more viable propulsion alternative they must become more scalable for use with very low thrust requirements such as in micro-satellites. A possible solution to this scalability issue is the use of ionization chambers composed of Micro Structured Electrode (MSE) Arrays [6, 7, 8]. This would potentially reduce these chambers to 20% or less of its current volume allowing for a great savings in mass and size, as well as a scaling down to much smaller thrust. Another benefit of using MSE arrays would be a reduction in power requirements. Ion engines currently require kilowatts of power and utilizing MSE arrays could decrease the power requirements into the hundreds-of-watt range, which would entail additional cost, size and weight benefits making them attractive for small satellites due to reduced power supply requirements.

This thesis extends the work of References 7 and 8 to flow situations. MSE arrays are used as the ionizer section but no accelerator or neutralizer is included. Different configurations of MSE arrays are studied in a wide range of pressures from approximately 10 milli-Torr to 500 milli-Torr.

Chapter II covers the equipment setup used for the experiments and offers a description of the MSE wafers used. Chapter III covers ion engine theory, both current and with MSE array theory. The ionization theory deals with the

breakdown process at various pressures and the method to sustain discharges. Chapter IV covers data and results of the testing of the MSE arrays. The fifth and sixth chapters will draw conclusions and make recommendations for future studies.

The use of MSE arrays is one alternative to the current ion-engine-ionization-chamber technology. The system tested in this work is limited in that different electrode materials, surface conditioning, array geometries, and alternate inert gases are not investigated. This work concentrated on the breakdown voltage as a function of electrode/hole geometry and gas pressure. The flow was caused by pressure differentials across the wafers but no attempt has been made to quantify the propellant flow or the degree of ionization.

THIS PAGE INTENTIONALLY LEFT BLANK

# II. EXPERIMENTAL APPARATUS

## A. VACUUM CHAMBER AND ASSOCIATED EQUIPMENT

The primary test apparatus for this work consists of a stainless steel/glass/Plexiglas vacuum chamber, two roughing pumps, a turbo-molecular vacuum pump, an argon supply system, high voltage DC power supply, and various metering equipment such as a volt meter, ammeter, oscilloscope, as well as hardware-to-software interface to record data using LabView™. The vacuum chamber is cylindrically shaped glass chamber resting on a rubber gasket on the stainless steel surface of the turbo-molecular pump housing. The top of the cylinder has an additional rubber gasket on which a removable thick Plexiglas disc rest to close the chamber. A gate valve in the stainless steel housing isolates the lower roughing pump and turbo-molecular pump from the chamber. The lower stainless steel surface contains multiple ports for positioning monitoring equipment to measure chamber pressure, and for providing suction for the other roughing pump, see Figures 3 and 4.

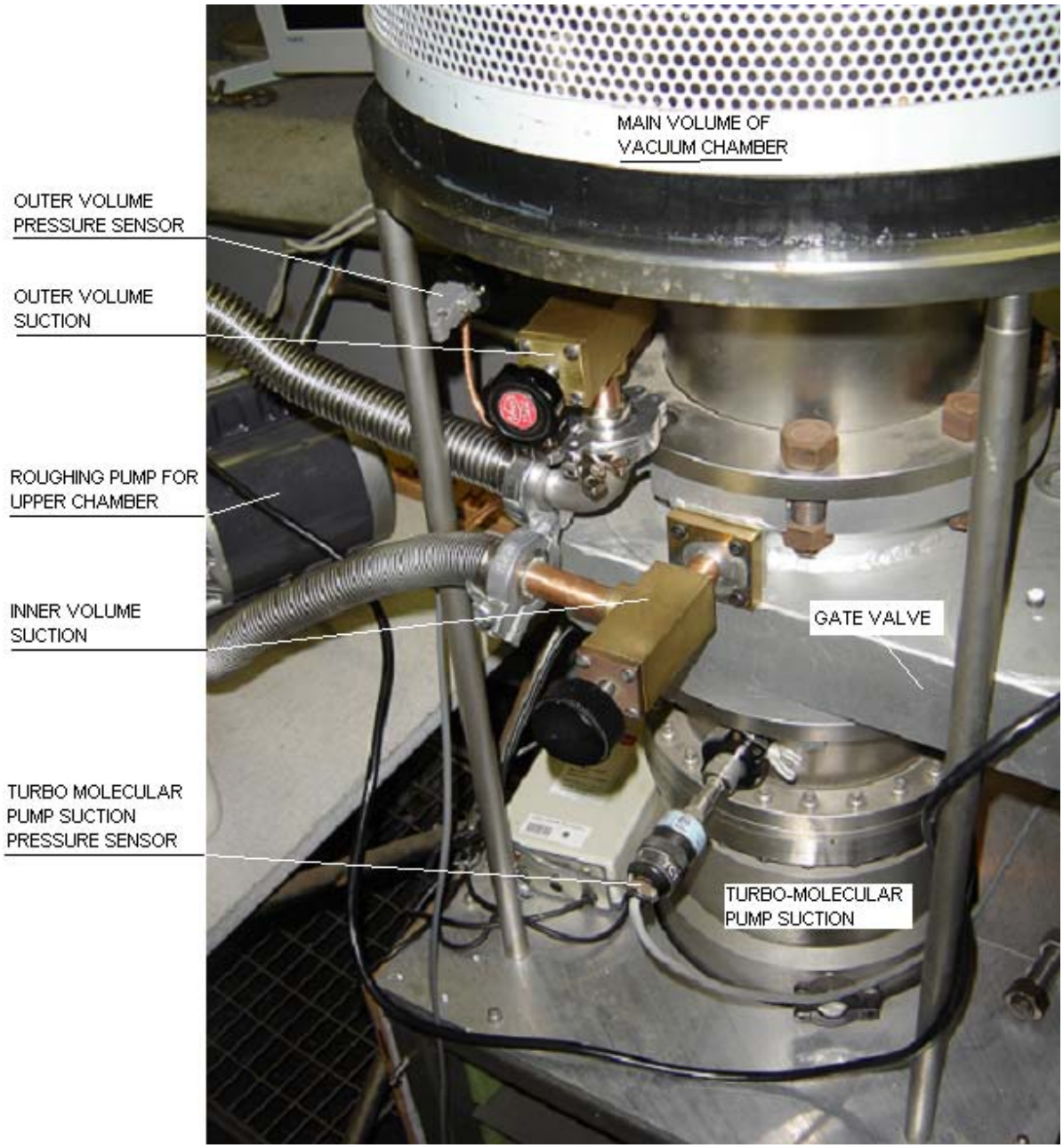


Figure 3. Lower Portion of the Testing Apparatus.

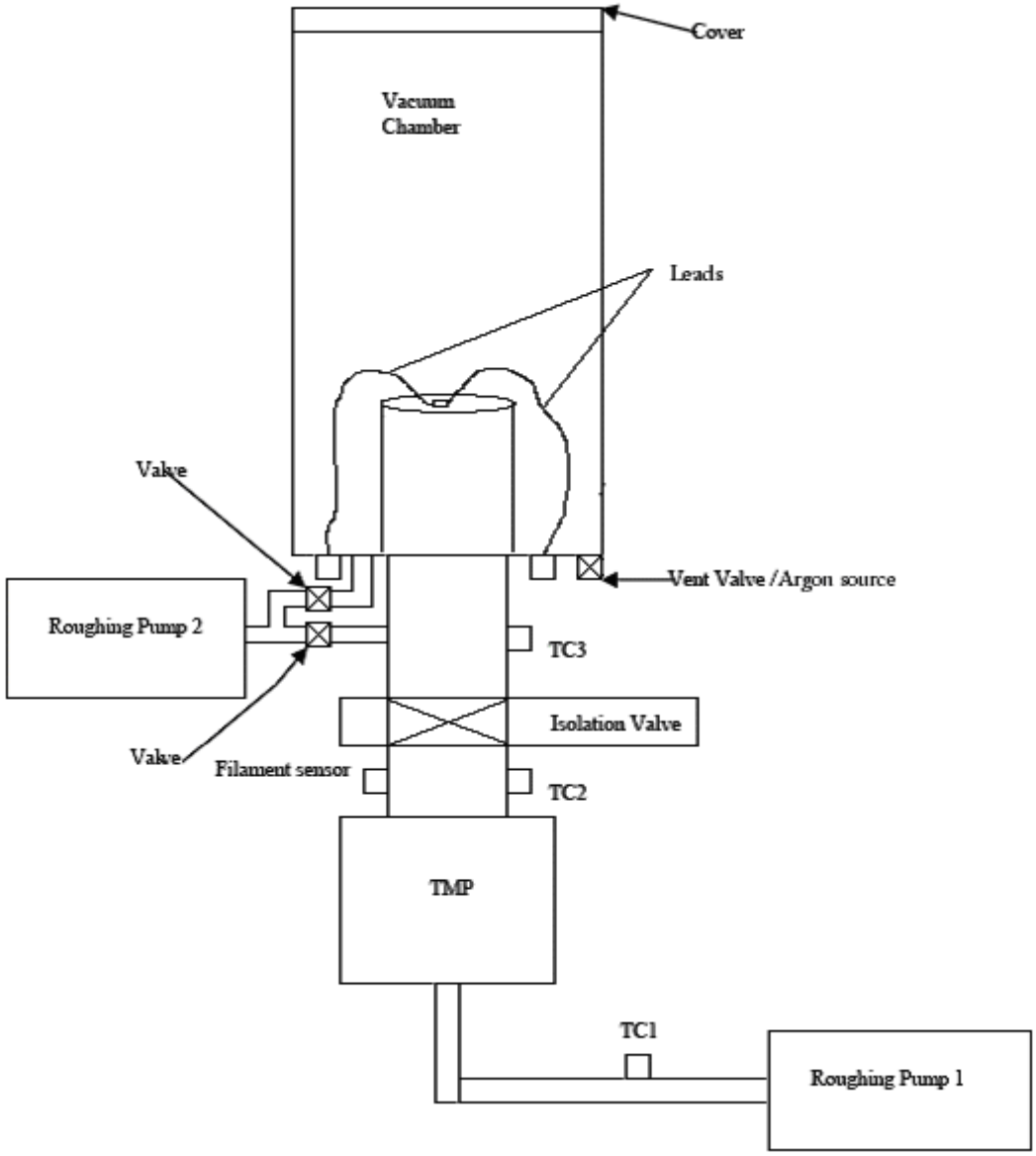


Figure 4. Diagram of vacuum chamber assembly and equipment

Figure 3 shows the lower portion of the vacuum chamber and the two sections of the second roughing pump as well as the gate valve used for isolation and throttling the flow.

The inner Plexiglas mounting platform and cylinder is used to establish a seal for creating a differential pressure, which induces flow of argon through the holes in the wafers. This is shown in Figure 5.

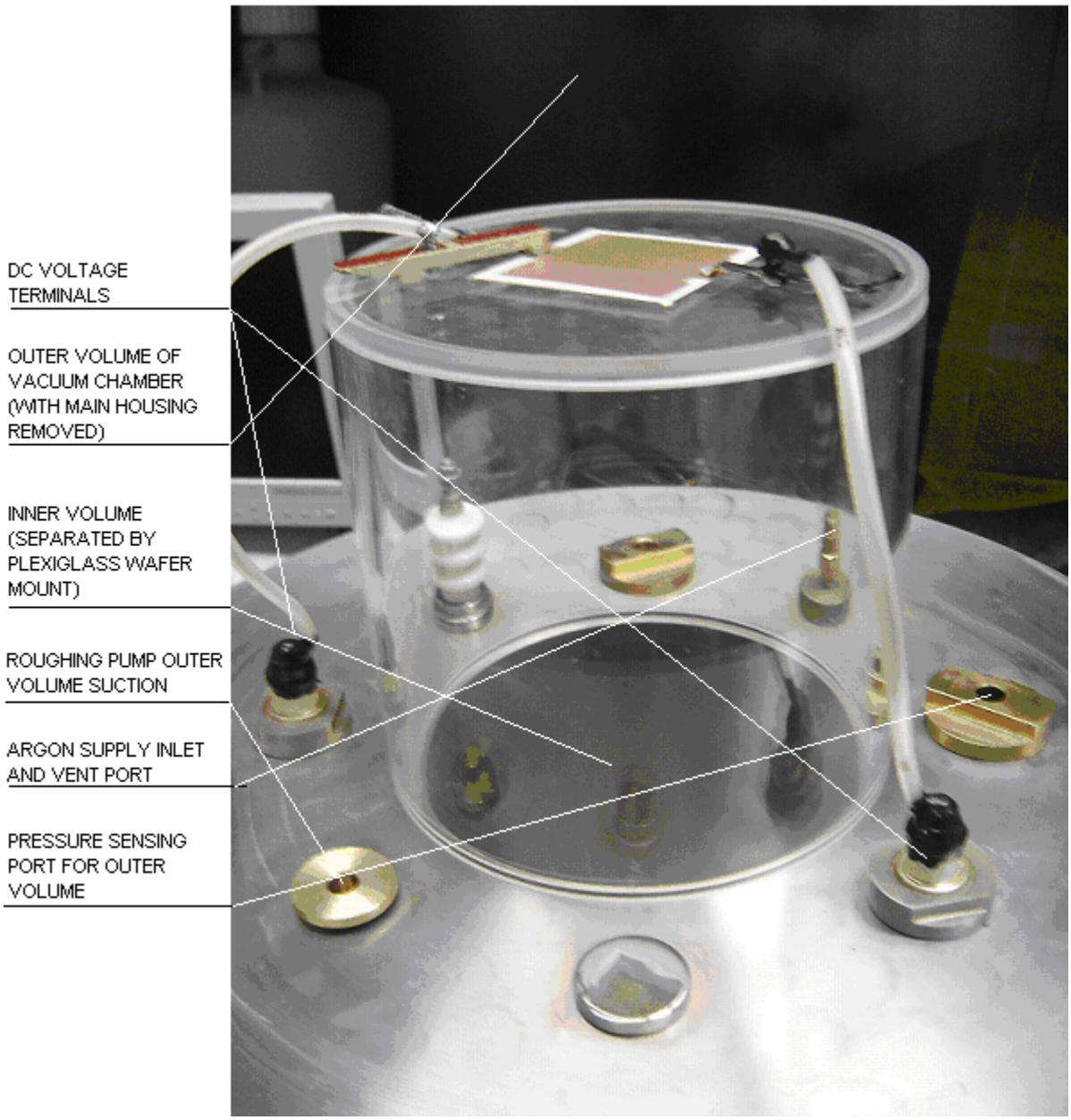


Figure 5. Plexiglas Wafer Mounting Structure.

Rubber O-rings seal the upper and lower portion of the mounting structure to ensure that the only flow path for the argon gas is through the MSE array, the wafer mounted to a recess on top of the structure. The vacuum chamber housing seen in Figure 3 and 4 encloses this mounting during operations establishing inner and outer pressure region for the wafer being tested. The argon is fed to the outer region and flows down to the inner region by the action of the turbo-molecular pump.

For start up sequence and operating procedures refer to the Appendix where equipment diagrams are included.

Once the turbo-molecular pump is engaged and draws vacuum down to the range of $10^{-6}$ Torr the chamber is filled with argon to the desired pressure and then the isolation valve is shut and the fill valve closed for no-flow testing. Flow testing is done similarly but instead of isolating the chamber the gate valve is used to throttle flow to the turbo-molecular pump thereby allowing a steady state to be reached with flow through the MSE array.

A variable DC power supply is used to adjust the voltage to the sample wafer in the chamber while breakdown voltage is monitored with an oscilloscope and a voltmeter.

Once breakdown is achieved the voltage is removed, and the system is either reset for the no flow testing or argon flow is throttled to a new pressure for the next flow testing.

## B. MICRO-STRUCTRED ELECTRODE ARRAY WAFERS

The MSE arrays used in these experiments are fabricated from a fiberglass laminate epoxy resin insulator sandwiched

between two layers of copper. The wafers are cut to approximately three inch by three inch pieces from large commercial sheets of material. These wafers are then drilled in the center with a five by five grid pattern using micro sized drill bits and a precision drill press. The holes are spaced so that they are two millimeters apart. Each wafer is then etched on the edges, using ferric chloride, to strip the copper from the edges preventing any current flow across them see Figure 6.

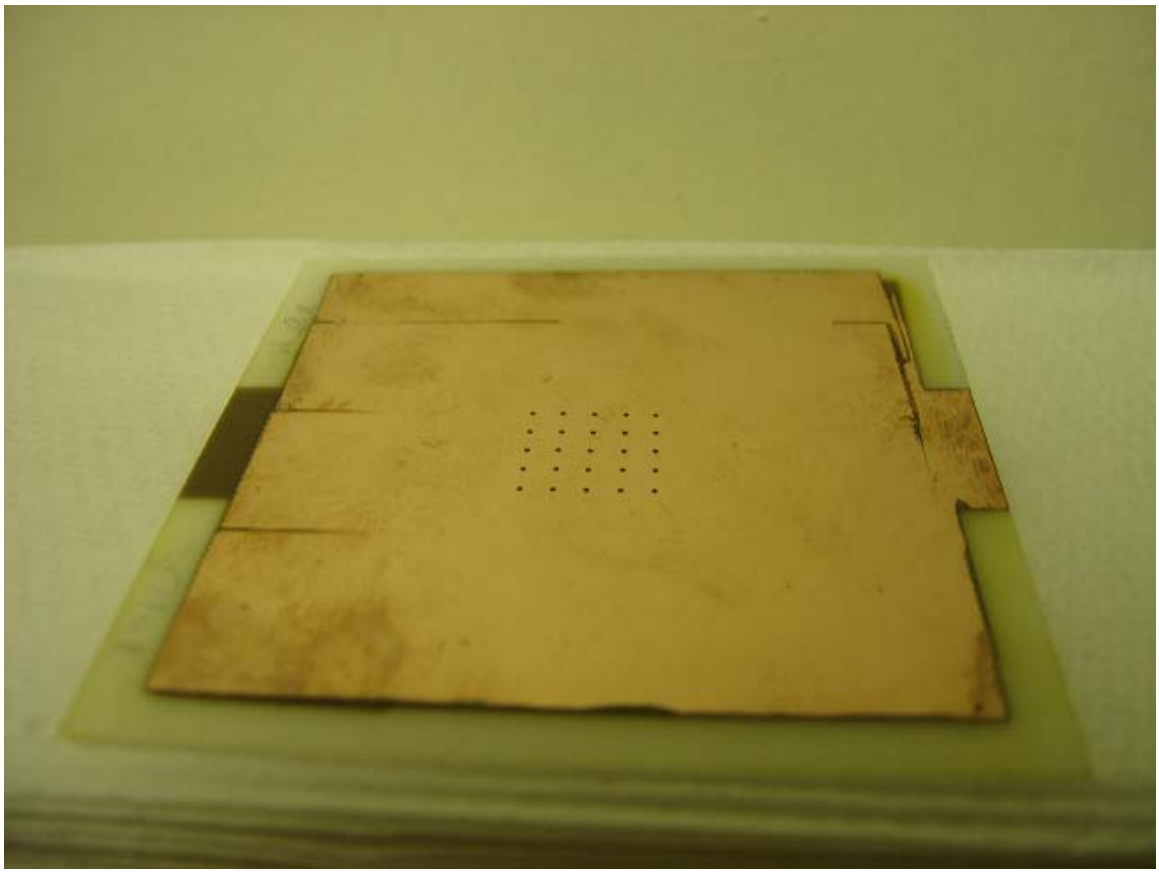

Figure 6. Copper Dielectric Copper Wafer with Holes and Etched Edges

Once etched, they are cleaned by immersion and rubbed down in an alcohol bath. Excess alcohol is then allowed to

evaporate. The wafer is then inspected and placed in its mounting position inside the vacuum chamber for experimentation as needed see Figure 5.

THIS PAGE INTENTIONALLY LEFT BLANK

# III. BACKGROUND OF IONIZATION CHAMBER MODIFICATIONS

## A. TOWNSEND THEORY OF BREAKDOWN

The geometry in the MSE arrays is used to enhance the local electric field when a voltage is applied to the electrodes. In the gaseous medium such as xenon or argon, the high electric field regions can cause free electrons to be amplified to an avalanche and a discharge is started [6].

When a sufficiently powerful electric field is applied to the array, breakdown occurs. Breakdown is the process where the non-conduction gas is converted to a conducting medium through ionization of the gas molecules.

From the Townsend theory of breakdown, we know that charge carriers are produced by volume/surface processes. This is described by the ionization coefficient $\alpha$, and by secondary emission coefficient $\gamma$. A self-sustaining discharge is started by having every electron that is lost at the anode replaced by either one generated at the cathode or through ionization of the gas in the chamber. The ionization coefficient depicts how electrons multiply in the direction of the electric field. The secondary emission coefficient depicts the electrons produced at the cathode-gas interface [9].

At low pressures the primary mode of electron production is by ion impact on the cathode surface. The breakdown voltage can be shown, in Equation (1), to depend on gas density (or pressure) and electrode separation:

$$V_b = \frac{Bpd}{\ln(pd) + \ln(\frac{A}{\ln(1+\gamma^{-1})})} \quad (1)$$

where $p$ is the pressure of the gas in Torr, $d$ is the distance between "parallel-plate anode and cathode" in cm, $A$ and $B$ are constants that vary for each gas medium [9]. Graphically this is represented by a Paschen curve, which depicts the breakdown voltage versus pressure multiplied by distance ($pd$) as shown by plotting the generalized form, Figure 7, of Equation 1, Equation 2.

$$Y = \frac{X}{\ln(X)} \quad (2)$$

Where Y represents the $V_b$ and X $pd$.

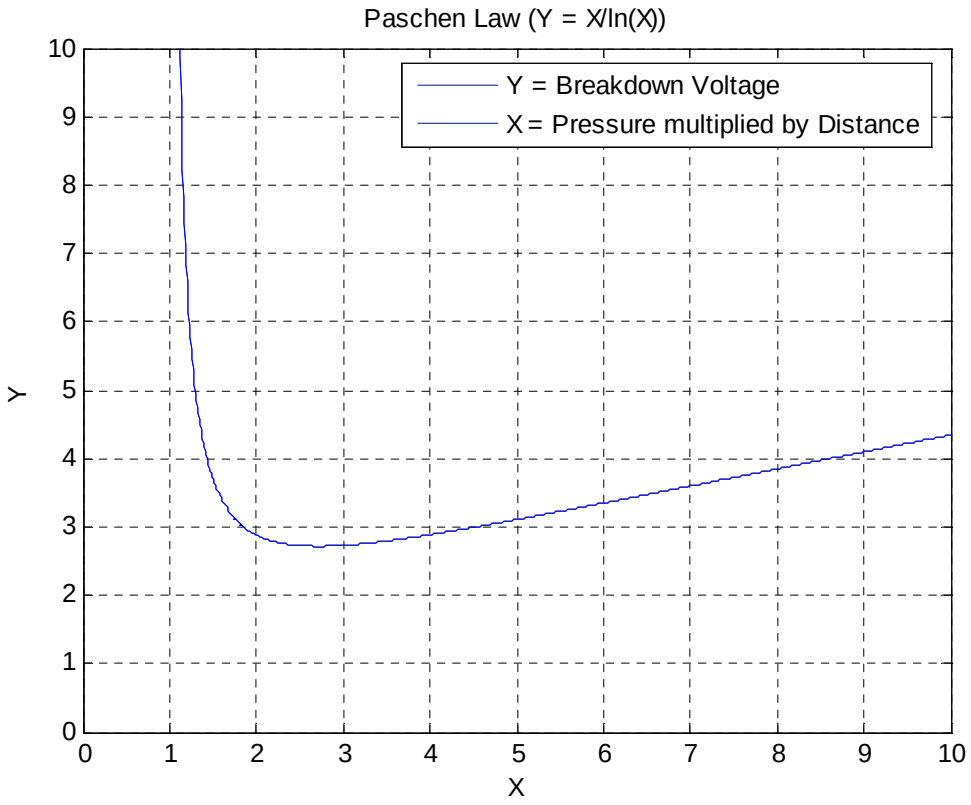


Figure 7. Generalized Paschen Curve.

On the left side of the Paschen curve, the breakdown voltage decreases rapidly as the $pd$ increases due to the initial low possibility of ionizing collisions which requires a strong electric field; this voltage decreases as the likelihood of collision increases with $pd$. A minimum is then reached and the voltage rises slowly as the probability of electrons creating secondary ionizations increases with $pd$. This minimum breakdown voltage is what is explored in this thesis in connection with the new electrode geometries of the ionization chamber.

One of the limitations of using equation 2 is the geometric differences between the MSE array and a parallel plate anode-cathode configuration. The set of holes differ also in that many parallel paths for breakdown are available and that each hole electrode shape is slightly different.

## B. MSE ARRAY GEOMETRY

Using MSE arrays geometry it is expected that a local enhanced electric field can be generated within the hole structures at relative low voltages. It is expected that the field will have additional non-uniformities due to imperfections in the individual holes. High electric fields are desired to generate cathode electron emission and produce the argon plasma [6].

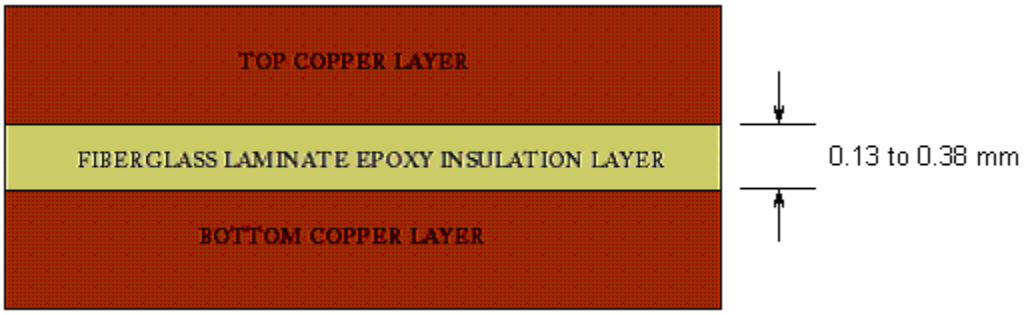


Figure 8. Cross-sectional view of Cu-dielectric-Cu layers in the Undrilled Wafer.

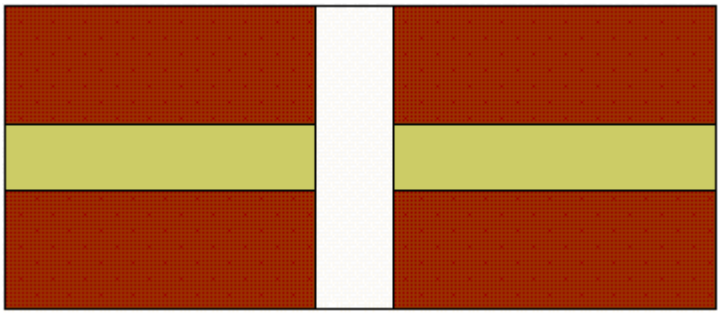

Figure 9. Cross-sectional view of layers with micro hole structure (holes are 0.300mm or 0.500mm in diameter.)

The MSE array geometry used is a five-by-five grid of holes in a three-inch by three-inch structure of two copper layers as described earlier. The copper layers are the electrodes. Figures 8 and 9 depict the wafers cross-sectional view. Each of the 25 holes can be a source of a micro-discharge that takes place during experimentation. The insulations layers used for this work consists of four units with two sizes of holes as described in the next section.

## C. FIELD EMISSION

Field emissions together with secondary emissions are the processes by which electrons are liberated from a cold surface under the effect of an electric field. These electrons are then accelerated in the field and collide with

neutral particles, in this case argon atoms. During ionizing collisions electrons are stripped from the argon atom creating an ion and more electrons which continue the process. This results in a continuous self-sustaining discharge that may no longer requires the field emission electrons. Field emission electrons are the primary cause of the initial ionization.

The MSE array geometry concentrates the electric field in the hole area thereby lowering the voltages required compared to those of parallel plate electrodes. Further enhancement of the electric field may be possible with manufacturing improvements and carbon nanotube technology introduced at the cathode [5].

THIS PAGE INTENTIONALLY LEFT BLANK

# IV. EXPERIMENTAL RESULTS

## A. INTRODUCTION

The objective of these experiments was to measure the breakdown voltages at various pressures for the composite-structures of the two different thicknesses and with two different hole diameters (see Table 1.) The thickness refers to the thickness of the insulations layer between the copper layers for each composite structure. There were a total of four structures utilized in the experiments, a no-flow test was done for comparison to References 7 and 8 and a flow test was done with each microstructure.

Table 1. Composite Structure's Experimental Matrix

| 0.127 mm Insulation layer | 0.381 mm Insulation layer |
|---|---|
| 0.300 mm holes | 0.300 mm holes |
| 0.500 mm holes | 0.500 mm holes |

Each MSE unit was mounted inside the vacuum chamber on the housing in which the leads from the high voltage DC power supply was attached. Then the chamber was evacuated to approximated $10^{-6}$ Torr and filled with ultra-pure research grade argon (purity 99.995%) to the required experimental pressure. Depending on the test being done the chamber was either re-evacuated to $10^{-6}$ Torr or a new equilibrium flow state was established for the next pressure test. The breakdown voltage was determined by increasing the

applied voltage and monitoring the voltage on a Tektronix™ oscilloscope. Once breakdown voltage was achieved the voltage was recorded. (See Appendix A for detailed operational procedures.)

Once the data, on the breakdown voltages, were obtained for all microstructures for flow and no flow conditions they were written into MATLAB™ and graphed for analysis and comparison.

## B. COMPARISON OF PRESENT NO-FLOW DATA TO REFERENCES 7 AND 8

This experimentation was a continuation of the work completed in Jason Cooper's and Frank Perry's no flow experimentation in 2006. The data obtained for the same insulation layer thickness and hole size is compared using no argon flow as was done in their testing Figures 10 and 11.

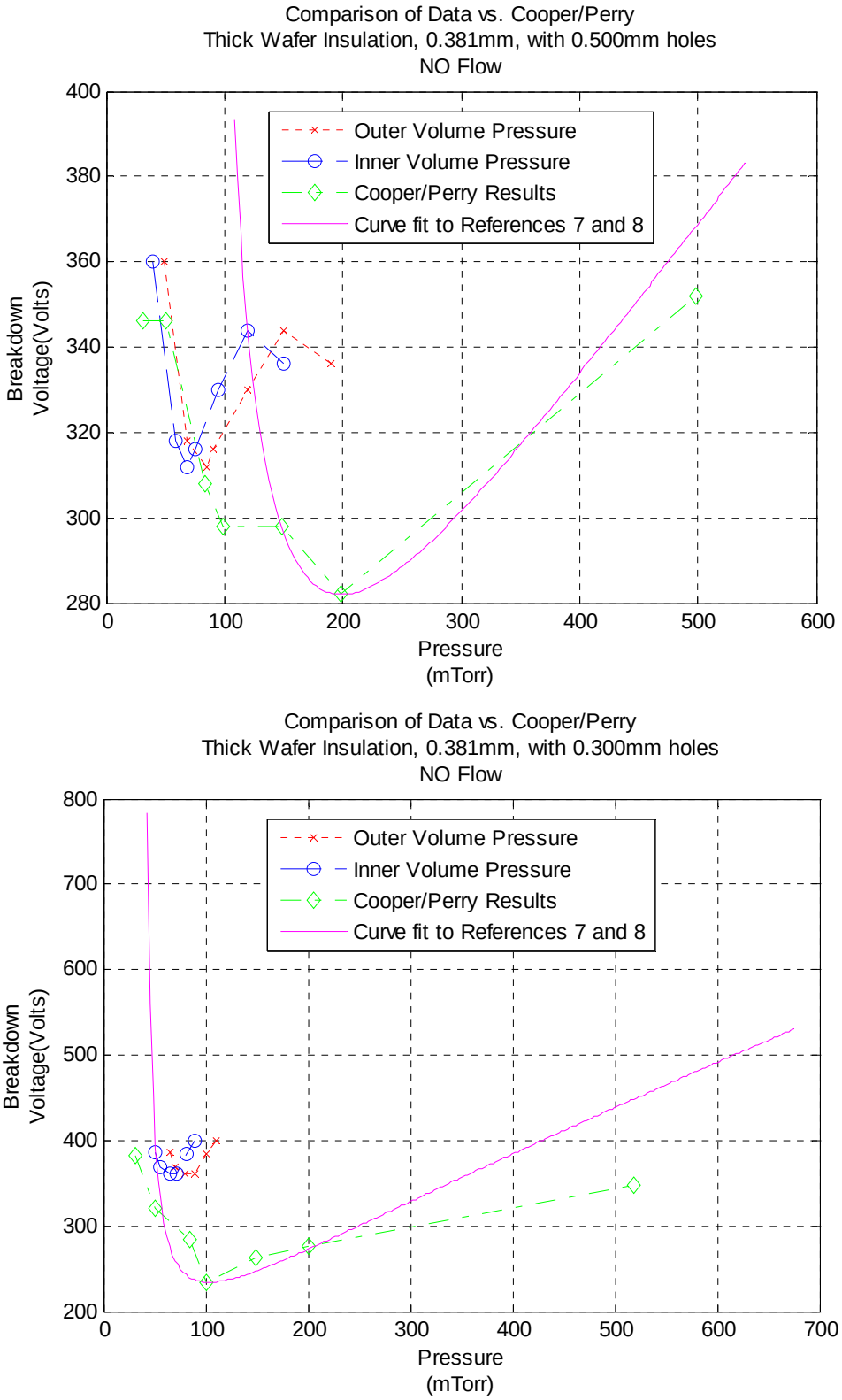


Figure 10. 0.381mm Insulation Layer No Flow Comparison

The new data for the thick wafer shows breakdown voltages taking place at a lower pressure but at a higher voltage than the results from References 7 and 8.

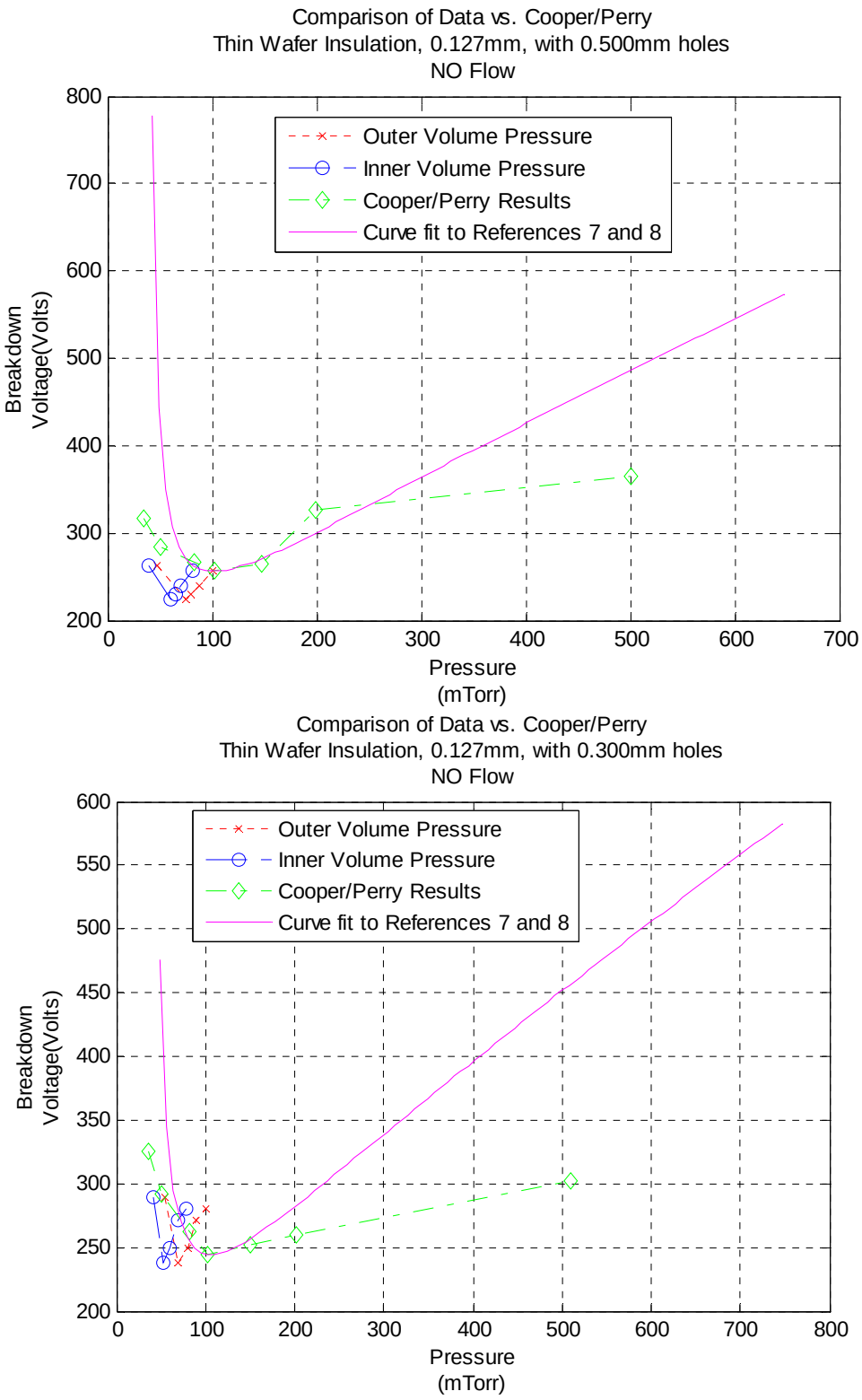


Figure 11. 0.127mm Insulation Layer No Flow Comparison

With the thin units, the breakdown voltages still occurred at lower pressures but the voltages were lower. Further testing might reveal if the thinner insulation layer is indeed more beneficial for the reduction in voltage necessary for breakdown.

The lower pressure experienced during the tests of each unit are likely caused by the change in experimental set up which is significantly different from that used in References 7 and 8, and the increase in the number of holes from the three-by-three hole array used in References 7 and 8 and the five-by-five hole array used in this work.

Both sets of figures are plotted against References 7 and 8 data as well as a Paschen curve fitted to their experimental results. Data is plotted only versus pressure due to hole diameter being the same for each case compared so the only variable is pressure. The two pressure readings from the present work are the inner and outer chamber pressure which even in the no-flow regime had a small difference (which can be due to instrument errors). The locations of the pressure sensing instruments in relation to the wafer surfaces should also have an effect.

## C. COMPARISON OF PRESENT NO FLOW DATA TO FLOW CONDITIONS

The no-flow data is now plotted against the flow data for the same wafer configuration for analysis and comparison seen in Figures 12, 13 and 14. The curves have been plotted voltage versus pressure and not pressure multiplied by distance for the same reasons noted in the previous section. Each voltage is plotted for both readings; the inner vacuum chamber volume, inside the Plexiglas mounting structure, and

the outer volume. Differences are minimal as noted previously for the no-flow conditions but are significant for the flow conditions because of the need to establish the differential pressure to create flow of argon through the MSE array holes. The data reveals that the inner chamber pressure during the flow regimes more closely correlates with the no-flow cases.

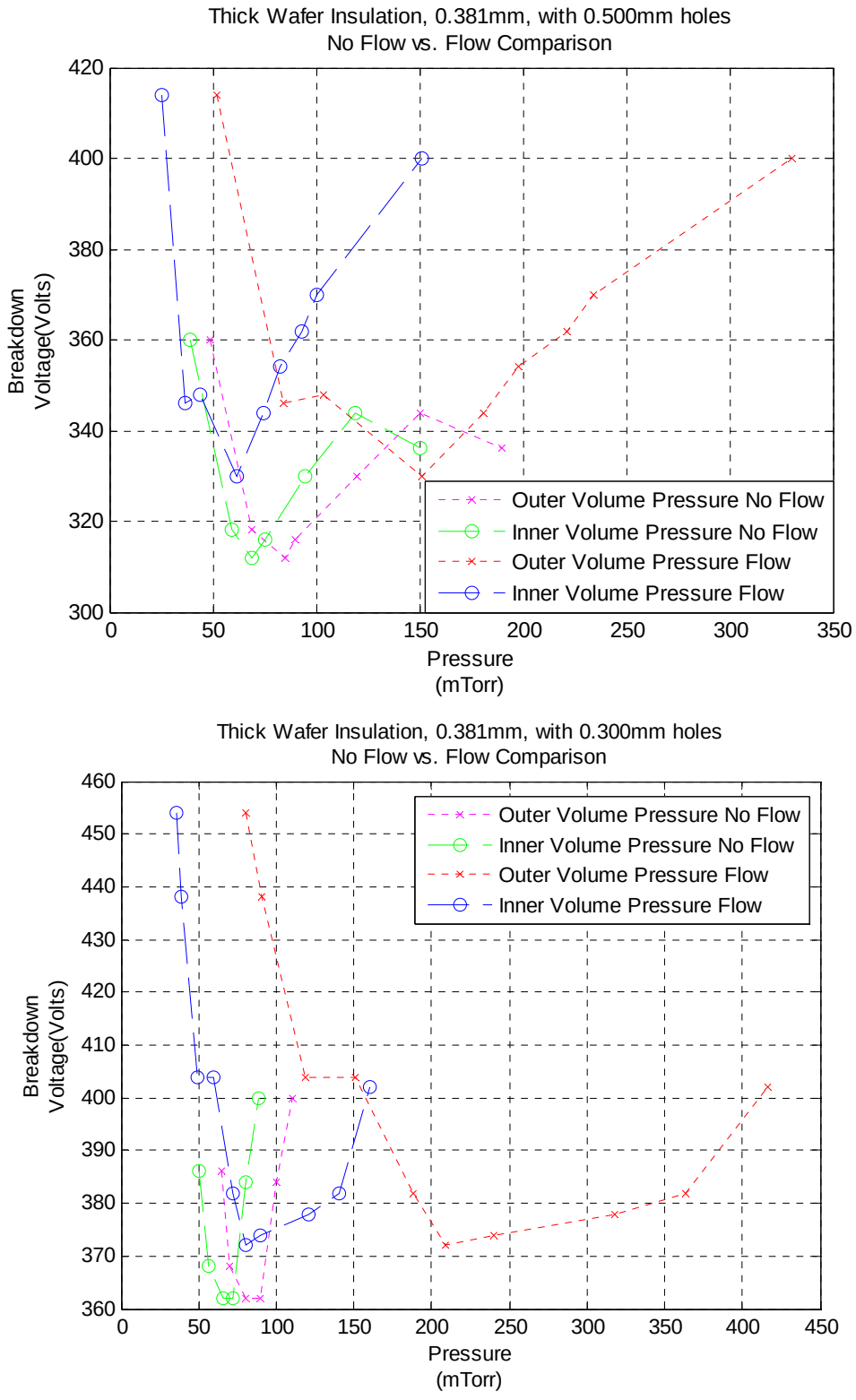


Figure 12. 0.381mm Flow vs. No Flow Comparison

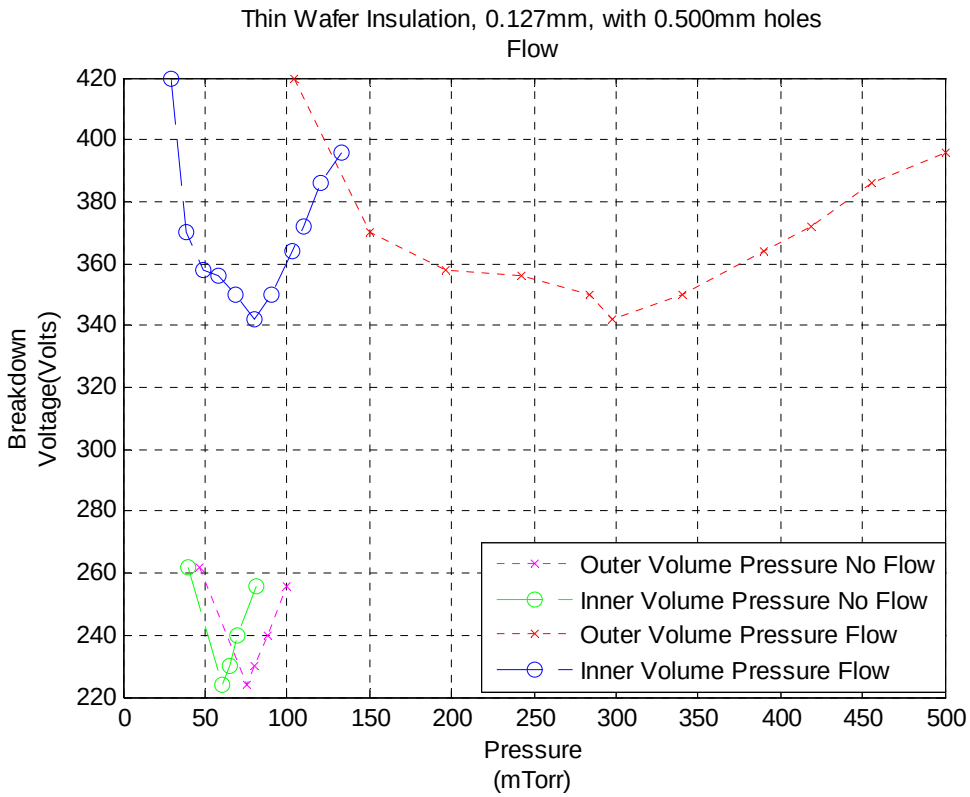


Figure 13. 0.127mm with 500mm holes Flow vs. No Flow Comparison

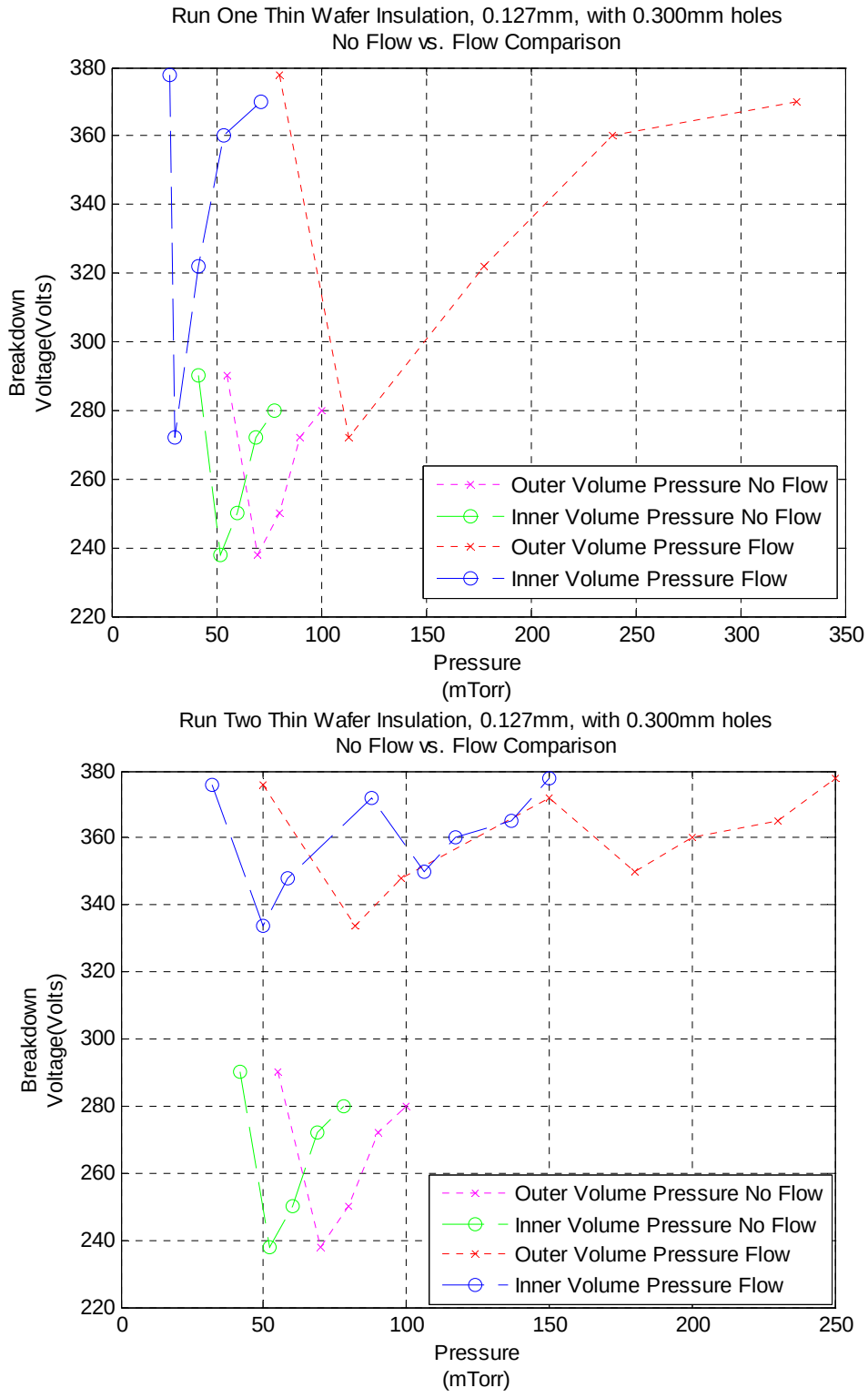


Figure 14. 0.127mm with 300mm holes Flow vs. No Flow Comparison

The key feature to note on the flow vs. no flow comparison is the breakdown voltages while occurring at a similar pressure, the inner chamber pressures correlated best, were significantly higher for the same MSE structure. This higher voltage with flow needs to be further studied to verify conditions at the array holes during testing. The second run in Figure 14 indicates a large variability of the flow case perhaps attributable to microstructure deterioration.

Another interesting point is that when the electrode polarity was reversed breakdown did not occur within our 500 volt limit see Figure 15.

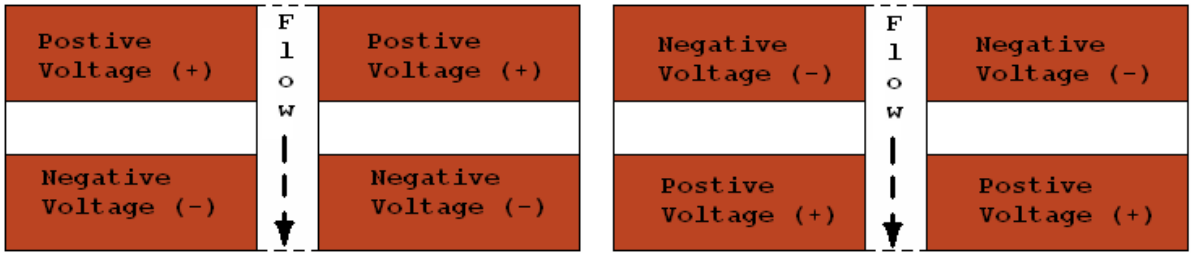


Figure 15. Polarities used for Testing

The image on the left in Figure 15 depicts the polarity used when breakdown was successfully achieved. The image on the right depicts the polarity when breakdown was not achieved within 500 volts.

## D. DETERIORATION

One of the significant unknowns of these experiments is the amount of deterioration of the electrodes during the runs and how that affects further testing of the same wafer. This deterioration changes the geometry of the electrodes,

over time. Deterioration is a function of time that the electrodes are under a discharge condition, the intensity of the discharge, and the material of the electrode. In this case copper was used to and the deterioration is noted in Figures 16 and 17. Based on the deterioration of the copper electrodes during breakdown, it is not a likely candidate for the final design.

The fabrication of the housing and mounting system for the arrays allowed testing flow situations for the arrays that were unable to be tested in the previous research.

The housing along with the fabrication of the MSE arrays was done with commonly used materials and manufacturing techniques, because a low cost method for conducting experiments was necessary. The sacrifices for this are the deterioration of the electrodes, and the limit of mechanical construction is reached with the 0.300mm diameter holes being drilled. The final material and manufacturing method would have to be chosen to prevent such degradation of the electrodes during discharge and the consistency in hole geometry so that each hole behaves the same under the same conditions.

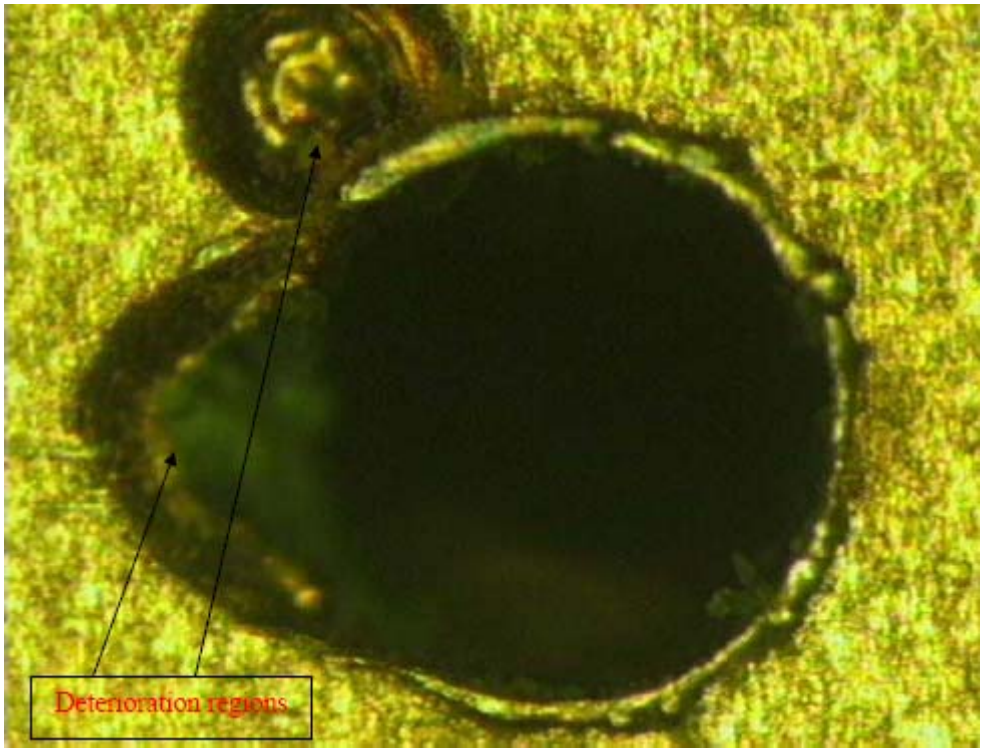


Figure 16. Photo of 0.300mm holes after testing. (References 7 and 8)

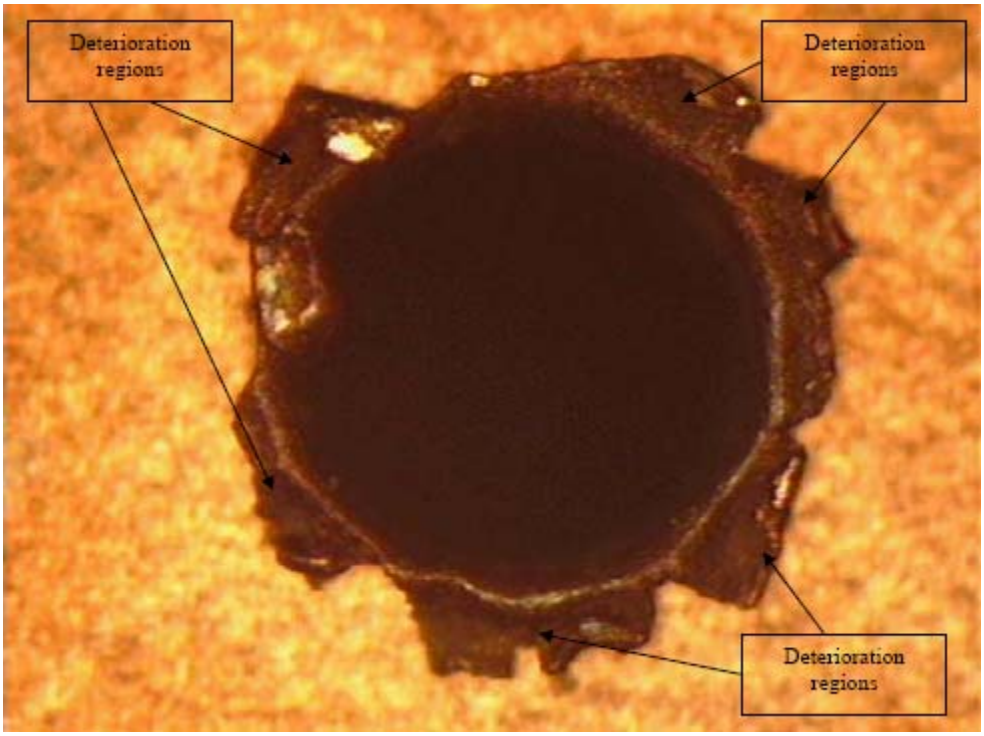


Figure 17. Photo of 0.500mm hole after testing. (References 7 and 8)

It is seen that there is significant deterioration of the electrodes after the ionization process in the argon has occurred. The amount of deterioration varies on holes size and the time that the hole was subjected to discharge conditions. It is clear that copper is not a suitable material for this application. Future study of materials and deterioration effects must be done to ensure a suitable conductor is used for the electrode materials. The refractory metals are known to be good candidates for ion thruster electrodes.

# V. CONCLUSIONS

This work shows that the ionization of argon, which is an alternate electric-propulsion fuel to xenon, can be achieved at low enough voltages by utilizing Micro-Structured Electrode (MSE) Arrays under flow and no-flow conditions. The MSE arrays serve to focus the electric fields and enhance the field emission effect for ionization. Minimum breakdown voltages between 230 and 350 volts at pressures around 80 milliTorr were consistently obtained with MSE arrays of 0.127 mm and 0.381 mm dielectric thickness each with 0.300mm and 0.500mm hole diameters. Each wafer tested had a 25 hole array; the holes were fabricated using conventional precision machining.

In the no-flow regime, pressure and voltage differences are noted between this work and the results of References 7 and 8. These are attributed mainly to the experimental set up and to the instrumentation. The addition of a pressure gage in the upper chamber added some uncertainty because of the thermocouple gage's low accuracy at the pressures of interest (±10 milliTorr). All electrical connectors were better insulated here and breakdown voltages were recorded manually as well as instantaneously with LabView™. The larger arrays probably added some uncertainties to these measured differences but care was taken to use the same materials, manufacturing techniques and testing procedures.

Flow results are more revealing. First, no breakdown was observed within a 500 volts limit when the polarity of the electrodes started negative with respect to the flow inlet, see Figure 15. With the negative electrode

downstream, breakdown voltages were observed which always exceeded their no flow counterparts and the flow voltage increases were larger for the thinner wafer (for 0.381 mm = +15 volts and for the 0.127 mm = +100 volts). The pressures recorded by the downstream thermocouple gage are more consistent with the no-flow data.

The effects observed with the flowing argon may be related to the motion of the ions. When ions have to move against a gas flow to reach the negative electrode, the electrical forces and the drag forces oppose each other and this seems to prevent breakdown at voltages below 500 volts. When the flow direction is towards the cathode voltage increases were observed which are less intuitive. Reference 10 reports on some calculations with argon in a similar geometry with similar pressures; his results show that the microdischarge acts as a pump inducing the discharge gas to flow towards the cathode at about 20 m/sec. Under our experimental conditions, the sonic speed of argon through the holes should be about 280 m/sec, so it is conceivable that flows much faster than 20 m/sec could disrupt the discharge dynamics and induce the observed higher voltages.

# VI. RECOMMENDATIONS

Several recommendations may be made from this study.

## A. REPEATABILITY STUDIES

Additional repeatability studies should be conducted on arrays manufactured with the same design. This would mitigate the deterioration issue somewhat and allow verification that breakdown can be achieved for the same array at approximately the same voltages.

## B. MATERIAL STUDIES

Alternate materials for the electrodes used for manufacturing the MSE arrays must be researched. A good conductor which would experience less pitting and degradation during discharge conditions should be investigated.

## C. STRUCTURE STUDIES

Circular holes were utilized for this study; other shaped holes and tapering of holes in the electrodes should be investigated for optimization of electric field generation and enhancing field emission effects.

## D. ENHANCED INSTRUMENTATION

Pressure measurements were taken far from the electrodes during experimentation. A redesigned housing and instrumentation system for the vacuum chamber would allow

for measurements to be taken in close proximity to the electrodes which would ensure that the pressure data gathered is sound.

## E. MULTIPLE ARRAYS IN SERIES

Study of percentage of ionization of the argon and the effect of multiple arrays in series should be done to maximize gas ionization thereby maximizing propellant used for thrust in an ion engine. In conjunction with this accurate flow rate of argon needs to be established and a current flow for measuring the amount of ions created to establish percent ionization.

# APPENDIX A. OPERATING PROCEDURES

## A. PROCEDURE FOR VACUUM CHAMBER OPERATION

Steps:

1. Ensure the gate valve isolating the turbo-molecular pump is closed.
2. Vent vacuum chamber to normal atmospheric pressure by opening vent valve.
3. Remove Plexiglas upper cover and place the wafer to be tested in the carriage seating area, ensure that the electrodes are in proper contact with the DC power supply leads.
4. Replace Plexiglas cover, and ensure vent valve is shut. Open isolations valves for the chamber roughing pump to begin drawing a vacuum.
5. Ensure power is supplied to the turbo pump, lower roughing pump, and instrument panel. Turn on the instrument panel and thermocouples gages ensure that TC2 (Figure 18) indicates 100 milliTorr or less then energize the turbo-molecular pump by pressing the yellow button and turn on filament gage.
6. Monitor chamber pressure once it reaches 100 milliTorr or less open the gate valve and shut the upper roughing pump isolation valves
7. Allow turbo-molecular pump to run until outer chamber pressure is less than 15 milliTorr.

8. Begin filling the chamber with argon to the desired pressure.

    a. For no flow testing shut the gate valve and the flow throttling valve and allow pressures to stabilize.

    b. For flow testing almost completely close the gate valve to throttle flow, throttle the argon flow valve to maintain equilibrium pressure.

## B. PROCEDURE FOR INSTRUMENT PANEL OPERATION

Steps:

1. Prior to energizing the DC power supply ensure that DC volts are set to zero.

2. Upon completion of Part A the experiment for that pressure is ready to be run. If not already done; energize the DC power supply, oscilloscope, voltmeter and ammeter. Verify that the ammeter is set to DC amps the default is DC volts upon startup.

3. Ensure LabView™ is running on the computer and the "john" model is open for data gathering. Under the window menu select schematic to bring up the diagram.

4. Start data gathering on LabView™ and then begin to raise voltage in a controlled manner on the power supply observing the oscilloscope for breakdown. Record breakdown voltage and stop data gathering in LabView™

5. Reduce voltage to minimum and then prepare the chamber for the next pressure to test at.

## C. DIAGRAMS

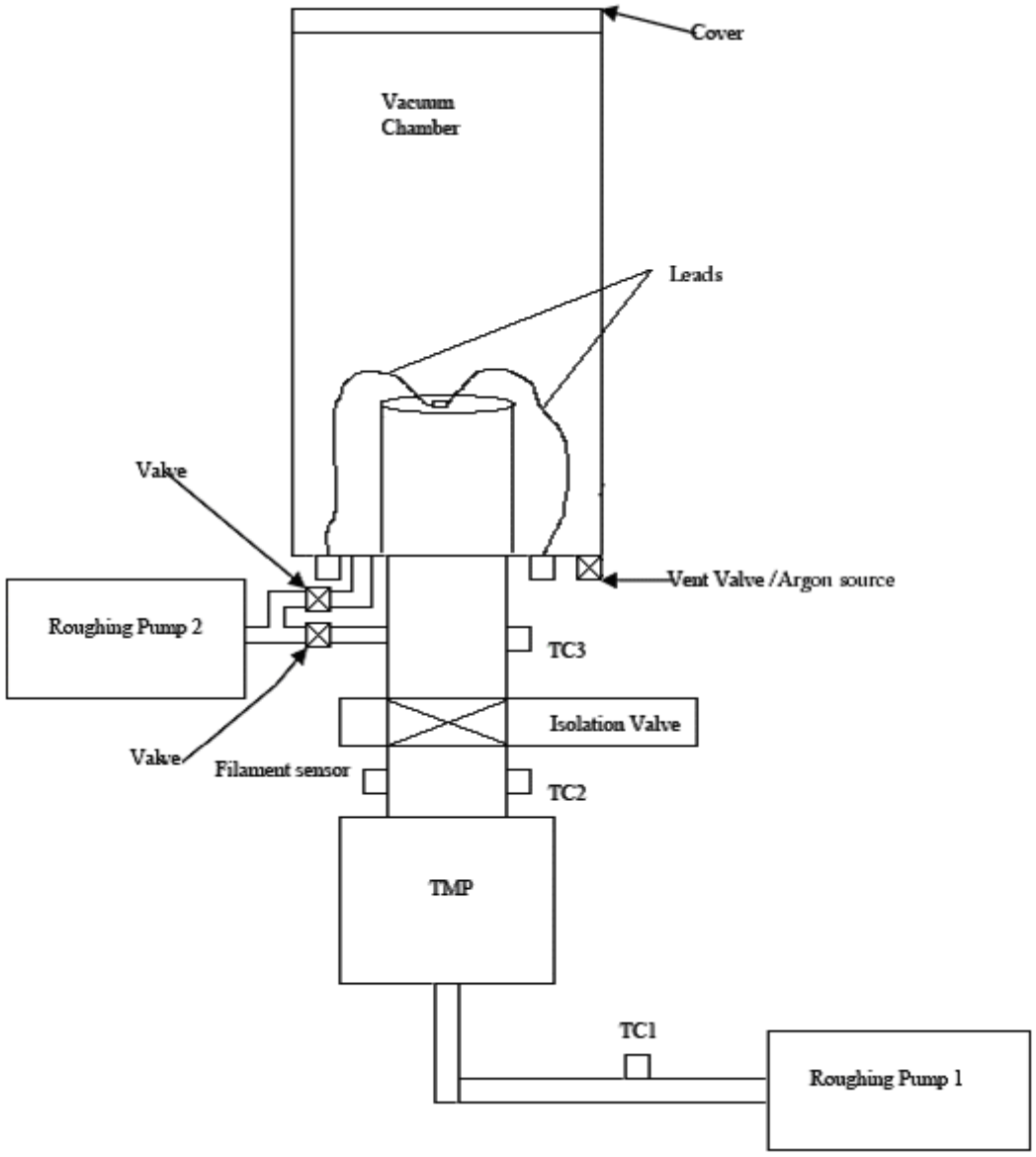


Figure 18. Diagram of vacuum chamber Assembly and Equipment.

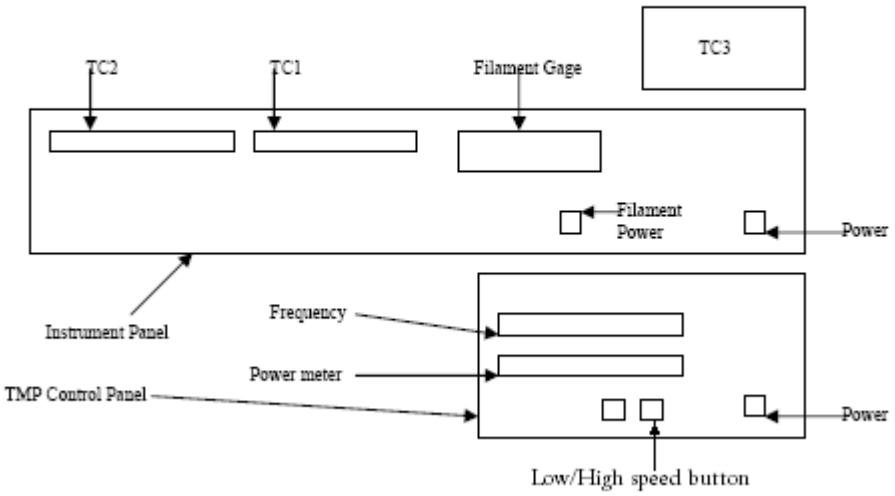


Figure 19. Control panel diagram for turbo-molecular pump

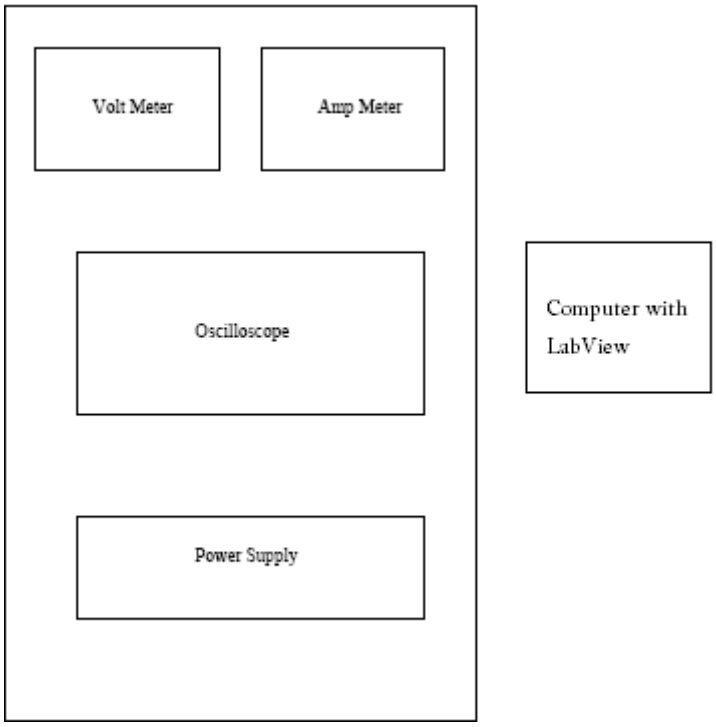


Figure 20. Equipment rack layout

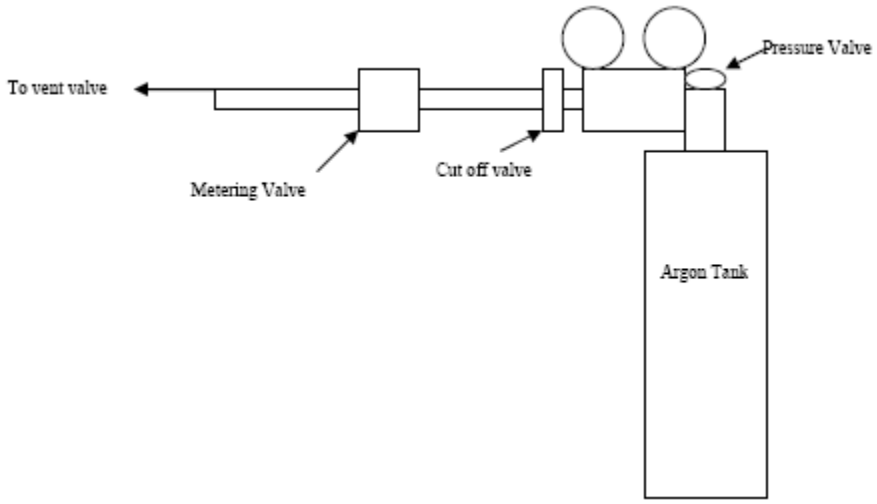


Figure 21. Argon supply system layout

# APPENDIX B. DATA TABLES

## A. DATA TABLES

### 1. Data from References 7 and 8 (9 Hole wafers)

Table 2. Thick insulation wafer with large holes

| 0.381mm Insulator with 0.500mm holes | |
|---|---|
| Pressure (milliTorr) | Breakdown Voltage (Volts) |
| 30.7 | 346 |
| 50.6 | 346 |
| 83.1 | 308 |
| 98.2 | 298 |
| 149 | 298 |
| 198 | 282 |
| 498 | 352 |

Table 3. Thick insulation wafer with small holes

| 0.381mm Insulator with 0.300mm holes | |
|---|---|
| Pressure (milliTorr) | Breakdown Voltage (Volts) |
| 32.2 | 382 |
| 50.7 | 320 |
| 84.1 | 284 |
| 100 | 234 |
| 149 | 262 |
| 200 | 276 |
| 518 | 348 |

Table 4. Thin insulation wafer with large holes

| 0.127mm Insulator with 0.500mm holes | |
|---|---|
| Pressure (milliTorr) | Breakdown Voltage (Volts) |
| 35.1 | 316 |
| 50 | 284 |
| 83.8 | 266 |
| 102 | 256 |
| 148 | 264 |
| 199 | 326 |
| 500 | 364 |

Table 5. Thin insulation wafer with small holes

| 0.127mm Insulator with 0.300mm holes | |
|---|---|
| Pressure (milliTorr) | Breakdown Voltage (Volts) |
| 35.2 | 326 |
| 51.3 | 292 |
| 82.2 | 262 |
| 103 | 244 |
| 151 | 252 |
| 202 | 260 |
| 509 | 302 |

## 2. No-flow Data from 25 Hole Wafers

Table 6. Thick insulation wafer with large holes

| 0.381mm Insulator with 0.500mm holes | | |
|---|---|---|
| Outer chamber pressure (milliTorr) | Inner chamber pressure (milliTorr) | Breakdown Voltage (Volts) |
| 49 | 39 | 360 |
| 69 | 59 | 318 |
| 85 | 69 | 312 |
| 90 | 75 | 316 |
| 120 | 95 | 330 |
| 150 | 119 | 344 |
| 190 | 150 | 336 |

Table 7. Thick insulation wafer with small holes

| 0.381mm Insulator with 0.300mm holes | | |
|---|---|---|
| Outer chamber pressure (milliTorr) | Inner chamber pressure (milliTorr) | Breakdown Voltage (Volts) |
| 65 | 50 | 386 |
| 70 | 56 | 368 |
| 80 | 65.5 | 362 |
| 90 | 72 | 362 |
| 100 | 80.7 | 384 |
| 110 | 89 | 400 |

Table 8. Thin insulation wafer with large holes

| 0.127mm Insulator with 0.500mm holes | | |
|---|---|---|
| Outer chamber pressure (milliTorr) | Inner chamber pressure (milliTorr) | Breakdown Voltage (Volts) |
| 47 | 40 | 262 |
| 75 | 60 | 224 |
| 80 | 65 | 230 |
| 88 | 70 | 340 |
| 100 | 81 | 256 |

Table 9. Thin insulation wafer with small holes

| 0.127mm Insulator with 0.300mm holes | | |
|---|---|---|
| Outer chamber pressure (milliTorr) | Inner chamber pressure (milliTorr) | Breakdown Voltage (Volts) |
| 55 | 41.5 | 290 |
| 70 | 52 | 238 |
| 80 | 60 | 250 |
| 90 | 69 | 272 |
| 100 | 78 | 280 |

### 3. Flow Data from 25 Hole Wafers

Table 10. Thick insulation wafer with large holes

| 0.381mm Insulator with 0.500mm holes | | |
|---|---|---|
| Outer chamber pressure (milliTorr) | Inner chamber pressure (milliTorr) | Breakdown Voltage (Volts) |
| 52 | 25.5 | 414 |
| 84 | 36.4 | 346 |
| 104 | 44.1 | 348 |
| 151 | 61.8 | 330 |
| 181 | 74.7 | 344 |
| 198 | 82.5 | 354 |
| 221 | 93.3 | 362 |
| 234 | 100 | 370 |
| 330 | 151 | 400 |

Table 11. Thick insulation wafer with small holes

| 0.381mm Insulator with 0.300mm holes | | |
|---|---|---|
| Outer chamber pressure (milliTorr) | Inner chamber pressure (milliTorr) | Breakdown Voltage (Volts) |
| 66 | 10.9 | No Breakdown |
| 80.5 | 36 | 454 |
| 91 | 39.1 | 438 |
| 119 | 49 | 404 |
| 151 | 60 | 404 |
| 188 | 72.2 | 382 |
| 209 | 80 | 372 |
| 240 | 90 | 374 |
| 318 | 121 | 378 |
| 363 | 140 | 382 |
| 416 | 160 | 402 |

Table 12. Thin insulation wafer with large holes

| 0.127mm Insulator with 0.500mm holes | | |
|---|---|---|
| Outer chamber pressure (milliTorr) | Inner chamber pressure (milliTorr) | Breakdown Voltage (Volts) |
| 45.3 | 13.1 | No Breakdown |
| 78.5 | 20.8 | No Breakdown |
| 104 | 28.9 | 420 |
| 150 | 38.2 | 370 |
| 197 | 48.4 | 358 |
| 242 | 58.6 | 356 |
| 284 | 68.2 | 350 |
| 298 | 80 | 342 |
| 340 | 90.2 | 350 |
| 390 | 103 | 364 |
| 419 | 110 | 372 |
| 456 | 120 | 386 |
| 500 | 133 | 396 |

Table 13. Thin insulation wafer with small holes first run

| 0.127mm Insulator with 0.300mm holes first run | | |
|---|---|---|
| Outer chamber pressure (milliTorr) | Inner chamber pressure (milliTorr) | Breakdown Voltage (Volts) |
| 52 | 20.6 | No Breakdown |
| 80 | 27.5 | 378 |
| 113 | 30 | 272 |
| 178 | 41.8 | 322 |
| 239 | 54 | 360 |
| 327 | 71.5 | 370 |

Table 14. Thin insulation wafer with small holes second run

| 0.127mm Insulator with 0.300mm holes second run | | |
|---|---|---|
| Outer chamber pressure (milliTorr) | Inner chamber pressure (milliTorr) | Breakdown Voltage (Volts) |
| 49.8 | 32.1 | 376 |
| 82.1 | 49.9 | 334 |
| 98.3 | 58.5 | 348 |
| 150 | 87.6 | 372 |
| 180 | 106 | 350 |
| 200 | 117 | 360 |
| 230 | 137 | 365 |
| 250 | 150 | 378 |

THIS PAGE INTENTIONALLY LEFT BLANK

# APPENDIX C. MATLAB™ CODE

## A. MATLAB™ CODE USED TO PLOT DATA FOR COMPARISON TO REFERENCE 7 AND 8

```
%Thesis Data NO FLOW Comparison to Cooper/Perry

%John Armstrong

clear all

close all

clc

%Thick/Largholes NO Flow

THICKLO = [49 69 85 90 120 150 190];

THICKLI = [39 59 69 75 95 119  150];

THICKLB = [360 318 312 316 330 344 336];

CPTHICKLP = [30.7 50.6 83.1 98.2 149 198 498];

CPTHICKLB = [346 346 308 298 298 282 352];

plot(THICKLO,THICKLB,'rx:')

hold on

plot(THICKLI,THICKLB,'bo--')

plot(CPTHICKLP,CPTHICKLB,'gd-.')

pdmin = 198*.0372;            %Code for Expected Values

VBmin = 282;                  %

c2 = 2.718/pdmin;             %

c1 = VBmin*c2/2.718;          %

x = .004:.0001:.02;           %
```

```
x= x*1000;                                  %
vb = (c1.*x)./(log(x)+log(c2));             %
plot(x*27,vb,'m','linewidth',1)             %
legend ('Outer Volume Pressure', 'Inner Volume
Pressure','Cooper/Perry
Results','Expected','Location','Best')
Title ({'Comparison of Data vs. Cooper/Perry';'Thick
Wafer Insulation, 0.381mm, with 0.500mm holes';'NO Flow'})
xlabel ({'Pressure';'(mTorr)'})
ylabel ({'Breakdown';'Voltage(Volts)'})
grid on

%Thick/Smallholes No Flow
THICKSO = [65 70 80 90 100 110];
THICKSI = [50 56 65.5 72 80.7 89];
THICKSB = [386 368 362 362 384 400];
CPTHICKSP = [32.2 50.7 84.1 100 149 200 518];
CPTHICKSB = [382 320 284 234 262 276 348];
figure(2)
plot(THICKSO,THICKSB,'rx:')
hold on
plot(THICKSI,THICKSB,'bo--')
plot(CPTHICKSP,CPTHICKSB,'gd-.')
pdmin = 100*.0384;          %Code for Expected Values
VBmin = 234;                %
```

```
c2 = 2.718/pdmin;          %
c1 = VBmin*c2/2.718;                    %
x = .0016:.0001:.025;                   %
x= x*1000;                              %
vb = (c1.*x)./(log(x)+log(c2));         %
plot(x*27,vb,'m','linewidth',1)         %
legend ('Outer Volume Pressure', 'Inner Volume
Pressure','Cooper/Perry
Results','Expected','Location','Best')
Title ({'Comparison of Data vs. Cooper/Perry';'Thick
Wafer Insulation, 0.381mm, with 0.300mm holes';'NO Flow'})
xlabel ({'Pressure';'(mTorr)'})
ylabel ({'Breakdown';'Voltage(Volts)'})
grid on



%Thin/Largeholes NO Flow
THINLO = [47 75 80 88 100];
THINLI = [40 60 65 70 81];
THINLB = [262 224 230 240 256];
CPTHINLP = [35.1 50 83.8 102 148 199 500];
CPTHINLB = [316 284 266 256 264 326 364];
figure(3)
plot(THINLO,THINLB,'rx:')
hold on
```

```
plot(THINLI,THINLB,'bo--')

plot(CPTHINLP,CPTHINLB,'gd-.')

pdmin = 102*.0153;      %Code for Expected Values

VBmin = 256;                              %

c2 = 2.718/pdmin;                         %

c1 = VBmin*c2/2.718;                      %

x = .00066:.0001:.01;                     %

x= x*1000;                                %

vb = (c1.*x)./(log(x)+log(c2));           %

plot(x*65,vb,'m','linewidth',1)           %

legend ('Outer Volume Pressure', 'Inner Volume
Pressure','Cooper/Perry
Results','Expected','Location','Best')

Title ({'Comparison of Data vs. Cooper/Perry';'Thin
Wafer Insulation, 0.127mm, with 0.500mm holes';'NO Flow'})

xlabel ({'Pressure';'(mTorr)'})

ylabel ({'Breakdown';'Voltage(Volts)'})

grid on



%Thin/Smallholes NO Flow

THINSO = [55 70 80 90 100];

THINSI = [41.5 52 60 69 78];

THINSB = [290 238 250 272 280];

CPTHINSP = [35.2 51.3 82.2 103 151 202 509];
```

```
CPTHINSB = [326 292 262 244 252 260 302];
figure(4)
plot(THINSO,THINSB,'rx:')
hold on
plot(THINSI,THINSB,'bo--')
plot(CPTHINSP,CPTHINSB,'gd-.')
pdmin = 103*.0137;    %Code for Expected Values
VBmin = 244;          %
c2 = 2.718/pdmin;     %
c1 = VBmin*c2/2.718;  %
x = .00066:.0001:.01; %
x= x*1000;            %
vb = (c1.*x)./(log(x)+log(c2));         %
plot(x*75,vb,'m','linewidth',1)         %
legend ('Outer Volume Pressure', 'Inner Volume
Pressure','Cooper/Perry
Results','Expected','Location','Best')
Title ({'Comparison of Data vs. Cooper/Perry';'Thin
Wafer Insulation, 0.127mm, with 0.300mm holes';'NO Flow'})
xlabel ({'Pressure';'(mTorr)'})
ylabel ({'Breakdown';'Voltage(Volts)'})
grid on
```

## B. MATLAB™ CODE FOR FLOW VS NO FLOW CONDITIONS

```
%Thesis Data FLOW/No Flow Comparison
%John Armstrong
clear all
close all
clc
%Thick/Largholes
THICKLFO = [52 84 104 151 181 198 221 234 330];
THICKLFI = [25.5 36.4 44.1 61.8 74.7 82.5 93.3 100
151];
THICKLFB = [414 346 348 330 344 354 362 370 400];
THICKLO = [49 69 85 90 120 150 190];
THICKLI = [39 59 69 75 95 119  150];
THICKLB = [360 318 312 316 330 344 336];
plot(THICKLO,THICKLB,'mx:')
hold on
plot(THICKLI,THICKLB,'go--')
plot(THICKLFO,THICKLFB,'rx:')
plot(THICKLFI,THICKLFB,'bo--')
legend ('Outer Volume Pressure No Flow', 'Inner Volume
Pressure No Flow','Outer Volume Pressure', 'Inner Volume
Pressure','Location','Best')
Title ({'Thick Wafer Insulation, 0.381mm, with 0.500mm
holes';'No Flow vs. Flow Comparison'})
xlabel ({'Pressure';'(mTorr)'})
```

```
ylabel ({'Breakdown';'Voltage(Volts)'})
grid on

%Thick/Smallholes
THICKSFO = [80.5 91 119 151 188 209 240 318 363 416];
THICKSFI = [36 39.1 49 60 72.2 80 90 121 140 160];
THICKSFB = [454 438 404 404 382 372 374 378 382 402];
THICKSO = [65 70 80 90 100 110];
THICKSI = [50 56 65.5 72 80.7 89];
THICKSB = [386 368 362 362 384 400];
figure(2)
plot(THICKSO,THICKSB,'mx:')
hold on
plot(THICKSI,THICKSB,'go--')
plot(THICKSFO,THICKSFB,'rx:')
plot(THICKSFI,THICKSFB,'bo--')
legend ('Outer Volume Pressure No Flow', 'Inner Volume
Pressure No Flow','Outer Volume Pressure', 'Inner Volume
Pressure','Location','Best')
Title ({'Thick Wafer Insulation, 0.381mm, with 0.300mm
holes';'No Flow vs. Flow Comparison'})
xlabel ({'Pressure';'(mTorr)'})
ylabel ({'Breakdown';'Voltage(Volts)'})
grid on
```

```
%Thin/Largeholes
THINLFO = [104 150 197 242 284 298 340 390 419 456
500];
THINLFI = [28.9 38.2 48.4 58.6 68.2 80 90.2 103 110 120
133];
THINLFB = [420 370 358 356 350 342 350 364 372 386
396];
THINLO = [47 75 80 88 100];
THINLI = [40 60 65 70 81];
THINLB = [262 224 230 240 256];
figure(3)
plot(THINLO,THINLB,'mx:')
hold on
plot(THINLI,THINLB,'go--')
plot(THINLFO,THINLFB,'rx:')
plot(THINLFI,THINLFB,'bo--')
legend ('Outer Volume Pressure No Flow', 'Inner Volume
Pressure No Flow','Outer Volume Pressure', 'Inner Volume
Pressure','Location','Best')
Title ({'Thin Wafer Insulation, 0.127mm, with 0.500mm
holes';'Flow'})
xlabel ({'Pressure';'(mTorr)'})
ylabel ({'Breakdown';'Voltage(Volts)'})
grid on
%Thin/Smallholes 1
```

```
THINSFO1 = [80 113 178 239 327];

THINSFI1 = [27.5 30 41.8 54 71.5];

THINSFB1 = [378 272 322 360 370];

THINSO = [55 70 80 90 100];

THINSI = [41.5 52 60 69 78];

THINSB = [290 238 250 272 280];

figure(4)

plot(THINSO,THINSB,'mx:')

hold on

plot(THINSI,THINSB,'go--')

plot(THINSFO1,THINSFB1,'rx:')

plot(THINSFI1,THINSFB1,'bo--')

legend ('Outer Volume Pressure No Flow', 'Inner Volume
Pressure No Flow','Outer Volume Pressure', 'Inner Volume
Pressure','Location','Best')

Title ({'Run One Thin Wafer Insulation, 0.127mm, with
0.300mm holes';'No Flow vs. Flow Comparison'})

xlabel ({'Pressure';'(mTorr)'})

ylabel ({'Breakdown';'Voltage(Volts)'})

grid on



%Thin/Smallholes 2

THINSFO2 = [49.8 82.1 98.3 150 180 200 230 250];

THINSFI2 = [32.1 49.9 58.5 87.6 106 117 137 150];
```

```
THINSFB2 = [376 334 348 372 350 360 365 378];

THINSO = [55 70 80 90 100];

THINSI = [41.5 52 60 69 78];

THINSB = [290 238 250 272 280];

figure(5)

plot(THINSO,THINSB,'mx:')

hold on

plot(THINSI,THINSB,'go--')

plot(THINSFO2,THINSFB2,'rx:')

plot(THINSFI2,THINSFB2,'bo--')

legend ('Outer Volume Pressure No Flow', 'Inner Volume
Pressure No Flow','Outer Volume Pressure', 'Inner Volume
Pressure','Location','Best')

Title ({'Run Two Thin Wafer Insulation, 0.127mm, with
0.300mm holes';'No Flow vs. Flow Comparison'})

xlabel ({'Pressure';'(mTorr)'})

ylabel ({'Breakdown';'Voltage(Volts)'})

grid on
```

# LIST OF REFERENCES


[1] Wright, Mike, "ION PROPULSION: Over 50 Years in the Making,"[http://science.nasa.gov/newhome/headlines/prop06apr99_2.htm]. November 2007.

[2] Wikipedia, "Ion Thruster." [http://en.wikipedia.org/wiki/Ion_thruster]. November 2007.

[3] Sutton, G.P. and Biblarz, Oscar, ***Rocket Propulsion Elements***, VIIth Edition, Wiley, NY, 2001.

[4] J. R. Beattie, "XIPS Keeps Satellites on Track," The Industrial Physicist, American Institute of Physics, Vol. 4, No. 2, June 1998.

[5] Biblarz, Oscar and Sinibaldi, Jose, "Study of DC Ion Thrusters with Argon Propellants," JPC paper AIAA 2006-4670, Sacramento, CA, 2006.

[6] Penache, Maria C., "Study of High Pressure Glow Discharges Generated by Micro-Structured Electrode (MSE) Arrays," PhD Dissertation, Frankfurt am Main University, Germany, 2002.

[7] Cooper, Jason T., "Study of a Novel Ionizer Configuration for the Ion Thruster," Master's Thesis, Naval Postgraduate School, Monterey, CA, December 2006.

[8] Perry, Frank H., "Apparatus for Study of Ion Thruster Propellant Ionization," Master's Thesis, Naval Postgraduate School, Monterey, CA, December 2006.

[9] Nasser, Essam, ***Fundamentals of Gaseous Ionization and Plasma Electroncis,*** John Wiley & Sons, Inc., 1971.

[10] Kusher, Mark, "Modelling of microdischarge devices; plasma and gas dynamics", Journal of Physics D: Applied Physics, Vol 38(2005), pp 1633-1643.

THIS PAGE INTENTIONALLY LEFT BLANK

# INITIAL DISTRIBUTION LIST

1. Defense Technical Information Center
   Ft. Belvoir, VA

2. Dudley Knox Library
   Naval Postgraduate School
   Monterey, California

3. Head, Information Operations and Space Integration Branch, PLI/PP&O/HQMC
   Washington, DC

4. Professor Oscar Biblarz
   Department of Mechanical and Astronautical Engineering
   Naval Postgraduate School
   Monterey, CA

5. Professor Jose O. Sinibaldi
   Department of Mechanical and Astronautical Engineering
   Naval Postgraduate School
   Monterey, CA

6. Provost, Dr. Leonard Ferrari
   Naval Postgraduate School
   Monterey, CA

7. Dean of Research
   Research Office
   Naval Postgraduate School
   Monterey, CA